Exploring wide bandgap metal oxides for perovskite solar cells

S. S. Shin, S. J. Lee (iD), and S. I. Seok (iD)

COLLECTIONS

View Online   Export Citation   CrossMark

ARTICLES YOU MAY BE INTERESTED IN

Exploring wide bandgap metal oxides for perovskite solar cells ⓔⓟ

View Online Export Citation CrossMark

S. S. Shin,[1,a)] S. J. Lee,[1,a)] ⓘⒹ and S. I. Seok[2,b)] ⓘⒹ

AFFILIATIONS

[1] Advanced Materials Division, Korea Research Institute of Chemical Technology (KRICT), 141 Gajeong-ro, Yuseong-gu, Daejeon 34114, South Korea

[2] Department of Energy Engineering, School of Energy and Chemical Engineering, Ulsan National Institute of Science and Technology (UNIST), 50 UNIST-gil, Eonyang-eup, Ulju-gun, Ulsan 44919, South Korea

[a)] S. S. Shin and S. J. Lee contributed equally to this work.
[b)] Author to whom correspondence should be addressed: seoksi@unist.ac.kr

ABSTRACT

The heterojunction formed when wide bandgap oxides come into contact with perovskite solar cells is essential for high efficiency as it minimizes charge leakage along with charge separation and charge transfer. Therefore, the electrical and optical properties of wide bandgap oxides, including the bandgap, charge mobility, and energy level, directly determine the efficiency of perovskite solar cells. In addition, the surface properties of the wide bandgap oxide act as an important factor that determines the efficiency through the wettability and penetration of the precursor solution during perovskite layer deposition and long-term stability through the intimate interfacial bonding with the perovskite. Although a great variety of wide bandgap oxides are known, the number that can be used for perovskite solar cells is considerably reduced in view of the limitations that the light absorber (here, perovskite) for solar cells is fixed, and the oxides must be uniformly coated at low temperature onto the substrate. Herein, a review of the results from several broad bandgap oxides used in perovskite solar cells is presented, and a direction for discovering new photoelectrodes is proposed.

Metal oxides have received a lot of attention from scientists and researchers in a variety of fields over the past several decades because of their distinct properties as well as their superior chemical and thermal stability.[1,2] Their unique properties include a high dielectric constant; superconductivity; reactive electronic transition; and good electrical, optical, and electrochromic characteristics, stem from partially filled d-shells.[3–9] For these distinct properties, metal oxides have been widely applied to technological fields in the form of sensors, piezoelectric devices, fuel cells, catalysts, solar cells, etc.[10–16] In particular, the use of wide bandgap metal oxides in perovskite solar cells (PSCs) has been intensively studied.[17–22]

Inorganic-organic hybrid perovskite, with a chemical formula of ABX_3, where A is an organic cation, B is a metal cation such as Pb or Sn, and X is a halide anion, is a promising light-harvesting material because of its excellent optoelectronic properties along with its ease in fabrication and low cost.[23–31] These properties have enabled the rapid development of PSCs that employ halide perovskite as a light-harvesting layer, achieving a power conversion efficiency (PCE) as high as 23.3%.[32–37] However, for successful commercialization, there are still two issues that need to be solved−device performance and stability.[38]

For application to PSC, metal oxides must have a wide bandgap so that more light can reach the perovskite absorber. The wide bandgap metal oxides can play a variety of roles in PSCs. Wide bandgap metal oxides can be utilized as an electron transport material (ETM) or a hole transport material (HTM) in PSCs. Metal oxides serving as an ETM or HTM should satisfy the following requirements.[17,18,20,39] First, they should have suitable band alignment. In the case of an ETM,

the conduction band minimum (CBM) and valence band maximum (VBM) have to be lower than those of the perovskite absorber. In the case of an HTM, the VBM should be higher than that of the perovskite absorber; moreover, the CBM should also be higher than that of the perovskite absorber for facile transfer of holes in addition to the blocking of electrons from the perovskite absorber. Second, good charge mobility is necessary to transport charge carriers swiftly and suppress charge recombination within an ETM and HTM. Moreover, the crystallinity of metal oxides enhances the photovoltaic performance of PSCs.

Also, wide bandgap metal oxides have been introduced into the interfacial layer between the two constituents of PSCs to improve device performance and stability.[40-45] Han et al. demonstrated that MgO coated onto an ETM effectively retards charge recombination at the ETM/perovskite interface, thereby increasing the FF and open circuit voltage (V_{OC}) of PSCs.[40] Guarnera et al. employed an Al_2O_3 buffer layer sandwiched between the perovskite absorber and HTM for the purpose of protecting the perovskite from metal migration. As a result, the PSC retained its initial efficiency after 350 h of operation under simulated standard full-sun illumination.[41] Kaltenbrunner et al. improved the long-term stability in air under continuous illumination by introducing the Cr_2O_3/Cr interlayer underneath the metal electrode.[42] In addition, the ultrathin Al_2O_3 layer on the HTM formed by atomic layer deposition (ALD) can effectively prevent moisture from penetrating into the perovskite absorber, ultimately improving the ambient stability after 24 days of storage.[43]

Instead of an ETM, insulating wide bandgap metal oxides such as Al_2O_3,[46-49] ZrO_2,[50,51] and SiO_2[52,53] have been successfully implemented in PSCs. They function as a scaffold rather than as an ETM because of their higher CBM compared with that of the perovskite absorber. In this case, photo-generated electrons are transported through the perovskite itself and remain in the conduction band of the perovskite absorber, which can lead to exceptionally high V_{OC}.[49]

In this perspective, we will focus on wide bandgap oxides as ETMs in PSCs. We will briefly review the use and limitations of binary and ternary metal oxides as ETMs and describe the development of new metal oxides.

Figure 1(a) represents the conventional n-i-p architecture for PSCs consisting of five different layers—transparent anode (usually, FTO or ITO), ETM, light-harvesting perovskite material, HTM, and metal cathode. Among them, an ETM could contain a metal oxide compact layer or metal oxide mesoporous layer or both. A metal oxide compact layer is essential for hole-blocking by preventing the direct contact of the perovskite layer with the transparent anode.[54-56] Metal oxide mesoporous layers play a vital role in helping the formation of a homogeneous perovskite layer as a scaffold as well as
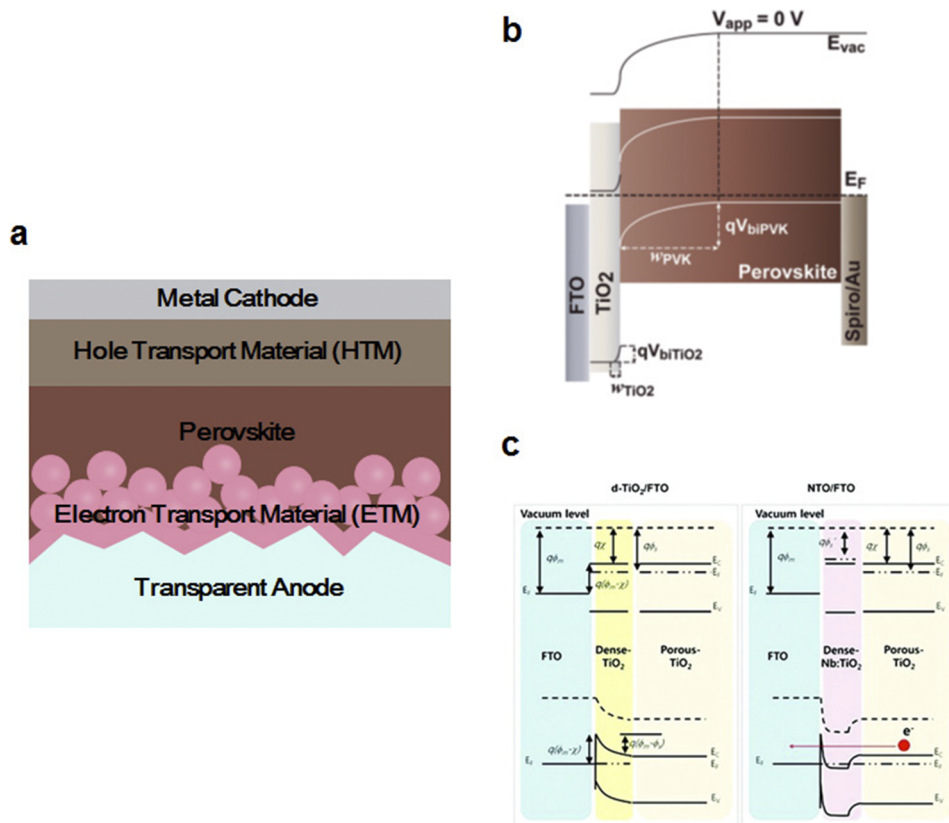
FIG. 1. (a) The common device architecture (n-i-p) of a PSC comprising electron transporting material (ETM), a perovskite absorber, a hole transporting material (HTM), and a metal contact. (b) Band diagram in equilibrium showing the formation of a perovskite-ETM heterojunction. The extension of the respective depletion zones and built-in voltages is indicated at each side. (c) Illustration of the band diagrams in the presence of the d-TiO$_2$ and Nb:TiO$_2$ layers before (upper) and after (under) contact.

inducing faster charge transfer from the perovskite absorber to the transparent anode due to its large contact with the perovskite layer.[52,56–58] For these reasons, many researchers have generally adopted the architecture consisting of both the metal oxide compact layer and mesoporous layer acting as an ETM to realize highly efficient PSCs, as described in Fig. 1(a).[34–36,59]

When an ETM forms a junction with perovskite materials or transparent conducting oxides (TCOs) for fabrication of PSCs, various requirements should be satisfied. First, when an ETM comes into contact with perovskite materials, a depletion zone is generated with a built-in potential (V_{Bi}) [Fig. 1(b)].[60,61] The built-in potential of the depletion zone is one of the important key parameters since it affects the internal electric field profile in the devices and also gives an upper limit for the V_{OC}.[61] Also, a built-in potential can suppress the back reaction of electrons from the ETM to the perovskite film, which assists in charge separation, charge transport, and collection.[62,63] Namely, a large built-in potential can lead to improved device performance with an increase in V_{OC}. Generally, the built-in potential corresponds to the difference in the work function (Fermi level) between the two sides (ETM and perovskite). Therefore, the shifting of Fermi levels in the ETM to a more negative potential is an effective strategy to increase the built-in potential between the ETM and the perovskite. Recently, some researchers changed the Fermi level of an ETM by surface modification, doping, and tuning of the particle size, resulting in a large improvement in V_{OC}.[62–64] Additionally, depletion widths are another important factor affecting device performance. Typically, total depletion widths can be determined by the following Eqs. (1) and (2).[60] Because contact equilibrium is assumed, the formation of depletion zones entails static values for the permittivity of each material,

$$W_{pvk} = \sqrt{\frac{2N_{ETM}\varepsilon_{pvk}\varepsilon_{ETM}(V_{bi} - V)}{qN_{pvk}(\varepsilon_{pvk}N_{pvk} + \varepsilon_{ETM}N_{ETM})}}, \quad (1)$$

$$W_{ETM} = \sqrt{\frac{2N_{pvk}\varepsilon_{pvk}\varepsilon_{ETM}(V_{bi} - V)}{qN_{ETM}(\varepsilon_{pvk}N_{pvk} + \varepsilon_{ETM}N_{ETM})}}. \quad (2)$$

In Eqs. (1) and (2), W_{PVK} and W_{ETM} are depletion widths of the perovskite and the ETM, respectively, q is the elementary charge, V is the applied voltage, ε_{pvk} and ε_{ETM} are the permittivity of the perovskite and the ETM, respectively, and N_{PVK} and N_{ETM} are doping densities of the perovskite and the ETM, respectively. Thus, the permittivity of metal oxides should be considered when selecting ETMs for PSCs. More importantly, the carrier concentration in metal oxides is a critical factor determining depletion widths. Generally, because the carrier concentration of metal oxides is higher than that of perovskite, the depletion region is dominant in the perovskite layer.[60] The increase in the carrier concentration by metal doping or control of oxygen vacancy can extend the depletion widths in the perovskite layer, which can improve charge separation at the ETM/perovskite interface.

Second, when an ETM comes into contact with a TCO (e.g., fluorine-doped tin oxide, FTO), a Schottky barrier, $q(\phi_m - \phi_s)$, can be formed [Fig. 1(c)].[65] Generally, a semiconductor and a metal contact (i.e., ETM/FTO contact) usually form the Schottky barrier, which occurs because of the difference in the work function between the metal (ϕ_m) and semiconductor (ϕ_s). The carriers need to overcome this barrier to be transferred from the semiconductor to the metal. In a dye-sensitized solar cell (DSSC), it has been reported that the efficiency can be improved by lowering the Schottky barrier.[65] Because a similar device architecture (i.e., FTO/compact metal oxide layer) is employed in PSCs, the removal or mitigation of Schottky barriers can be one of the key strategies to improve efficiency. The most effective approach to reduce the Schottky barrier is to dope the metal onto an ETM to change the work function of the ETM, leading to ohmic contact characteristics, which can facilitate electron transfer from the ETM to FTO through tunneling.

A metal-oxide-based ETM could be one of most important sources of device stability, including abnormal hysteresis, in PSCs.[66,67] Generally, metal oxides inevitably possess an oxygen vacancy or surface defect. During voltage scans, oxygen vacancies in the metal oxide can migrate under electric field; the accumulation of oxygen vacancies at the metal oxide/perovskite interface slows down electron extraction, causing anomalous hysteresis.[66] Additionally, it can influence the long-term stability of the device.[67] Recently, some researchers have proposed a surface modification strategy via chlorine or polymer-based defect passivation to reduce oxygen vacancy or defects in the metal oxide.[67,68] Prior to the commercialization of PSCs, however, more studies on device stability, including hysteresis, need to be performed.

TiO$_2$ is the most widely used ETM in PSCs. There are many well-known preparation methods and much information about the electrical, optical, and physical properties of TiO$_2$ because the use of TiO$_2$ in DSSCs has been extensively studied.[69] In 2009, Miyasaka's group first adopted TiO$_2$ as an ETM for the fabrication of liquid-type perovskite-sensitized solar cells with the same configuration as DSSC.[70] The PCE of the PSC was low at the time, but the solid-type HTM was first introduced to solve the rapid degradation of the perovskite by liquid electrolyte.[71] Although our group used an mp-TiO$_2$, we proposed a PSC with a new architecture in which the perovskite material fills all the mesoporous TiO$_2$ and exists as an overlay layer, while a hetero-junction is formed with hole-conducting poly(triarylamine).[72] With the aid of solvent engineering, mesostructured PSCs including dense, pin-hole-free perovskite films reached a certified PCE of more than 16% in 2014.[32] The following year, a PCE of greater than 20% was reported by tailoring the composition of perovskite.[33] Finally, reducing deep-level traps of perovskite materials yielded a certified PCE of over 22%.[35] To realize highly efficient PSCs, many researchers have constructed mesostructured PSCs using TiO$_2$ as an ETM.[34–36,73]

However, mesoscopic TiO$_2$ typically requires a high-temperature processing, which limits the application of plastic

substrates.[74] In addition, TiO_2 degrades perovskite materials under light illumination due to its photocatalytic properties and, thus, leads to inferior long-term photostability.[75] Moreover, TiO_2 has low electron mobility that can retard facile electron transport and increase charge recombination.[76] To solve these problems, many scientists have tried to find a new wide bandgap metal oxide that could replace TiO_2. The band alignment of various wide bandgap metal oxides, which have been adopted as ETMs in PSCs, is plotted in Fig. 2(a).

ZnO has been widely used as an ETM along with TiO_2 in DSSC due to its superior electrical and optical properties. Electron mobility of bulk ZnO is about 205-300 $cm^2 V^{-1} s^{-1}$, which is two orders of magnitude higher than that of TiO_2 (<1 $cm^2 V^{-1} s^{-1}$); this mobility can lead to facile electron

transport and then, subsequently, to reduced charge recombination. Also, ZnO can be fabricated without high-temperature processing. In 2014, the room-temperature-processed ZnO nanoparticulate film was employed via the spin-coating method, exhibiting a PCE as high as 15.7%.[77] In 2016, PSCs employing fully covered Al-doped ZnO by the sputtering method exhibited a PCE of 17.6% with a V_{OC} of 1.07 V.[78] However, PSCs with ZnO have trouble maintaining chemical stability because ZnO degrades perovskite materials on account of its basic nature. This fact has slowed down the development of ZnO-based PSCs.[79] Most recently, a ZnO-based planar PSC achieved a PCE greater than 21%, with improved stability, by the surface modification of ZnO nanoparticles.[80] Nevertheless, issues about the further enhancement of both stability and efficiency still remain for ZnO-based PSCs.
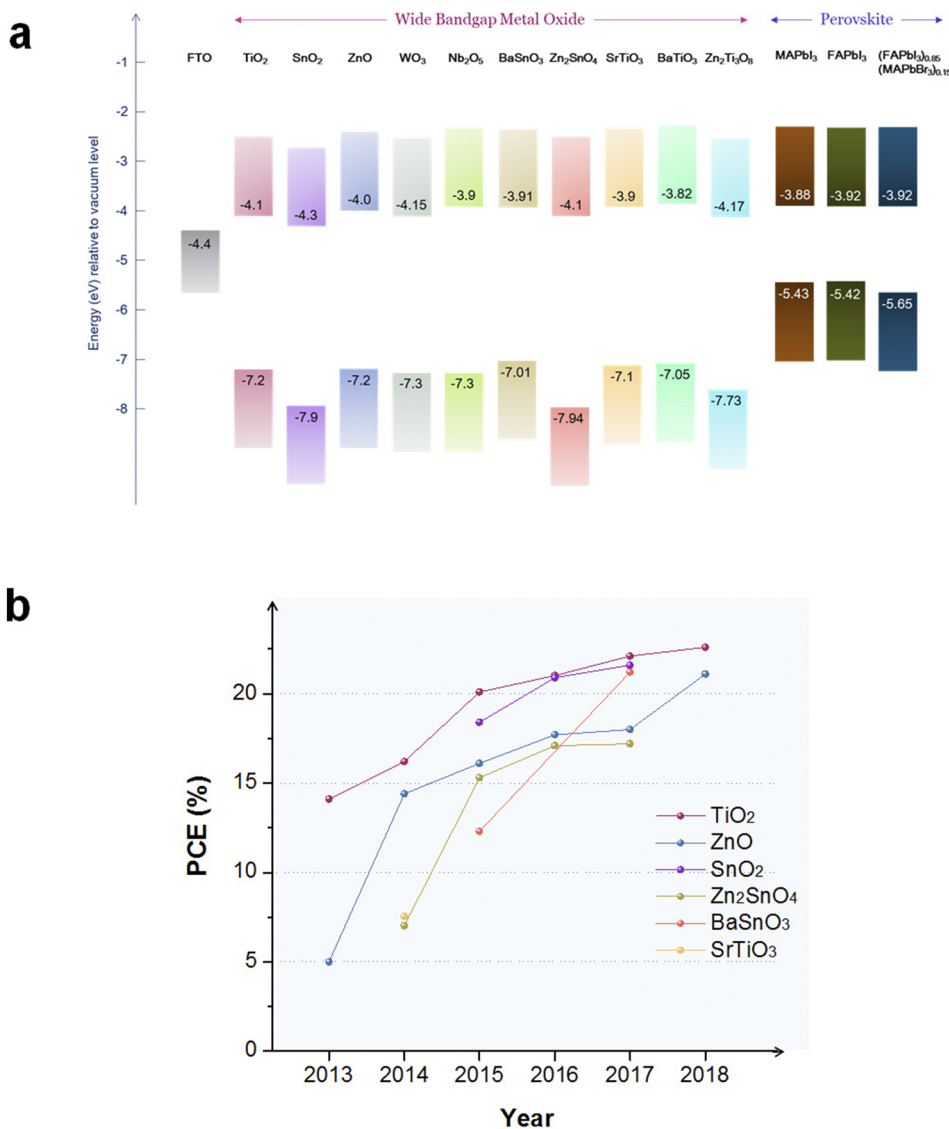
FIG. 2. (a) Energy-level diagrams of various wide bandgap metal oxides and perovskite absorbers used as ETM and light-harvesting material, respectively, in PSCs. (b) Evolution of PCE for PSCs employing various wide bandgap metal oxides as ETM.

In 2015, SnO_2 was raised as another alternative to TiO_2 in PSCs although it was not a notable material in DSSCs as much as TiO_2 or ZnO. Through low-temperature processing by ALD, Baena et al. successfully fabricated SnO_2-based planar PSCs with a PCE greater than 18%, with voltage exceeding 1.19 V, and excellent photostability.[81] They explained that SnO2 had a barrier-free energetic configuration at the energy level with perovskites. Anaraki et al. further improved the PCE of SnO_2-based planar PSCs up to ~21% via chemical bath deposition (CBD).[82] Lately, with the introduction of spin-coated SnO_2 nanoparticles, SnO_2-based PSCs have achieved considerable development with a certified efficiency of 20.9%.[83] SnO_2 as an ETM has gained much attention in the field of PSCs because of its favorable band structure, high electron mobility (240 cm^2 V^{-1} s^{-1}), wide optical bandgap, low-temperature processability, and chemical- and photostability.[21] Besides ZnO and SnO_2, various binary metal oxides such as WO_3,[84,85] Nb_2O_5,[86] In_2O_3,[87] and CeO_x[88] have been studied as ETMs of PSCs. We summarized the evolution of the PCE of PSCs based on various wide bandgap metal oxides over many years [Fig. 2(b)].

Doping is one of the most effective ways of modifying the electrical properties of wide bandgap binary metal oxides. According to theoretical study, the ideal gap of a CBM between an ETM and perovskite to obtain an optimum V_{OC} is in the range of 0.0–0.3 eV.[89] Some researchers reported that Mg-doped TiO_2[90,91] and Mg-doped ZnO[92] have the elevated CBM, which increases the charge recombination resistance, finally, the photovoltaic performance of the resulting PSCs with enhanced V_{OC}.

Ternary metal oxides can be attractive candidates, as their electrical properties and band structure can be easily modified by alternating the composition. In 2014, Bera et al. reported the fabrication of perovskite-structured $SrTiO_3$-based PSC with a PCE of 7%.[93] Subsequently, other Ti-based ternary metal oxides such as $BaTiO_3$ and $Zn_2Ti_3O_8$ have been studied, but their efficiency is quite low because of their inferior mobility and improper band alignment in relation to perovskite.[94,95] As another alternative, Sn-based ternary metal oxides have been addressed as the best candidates for ETMs in PSCs because the CBM of Sn-based oxides primarily originates from the Sn 5s–O 2p orbital interaction, giving rise to a large conduction band (CB) dispersion with low effective mass; lower effective mass results in higher electron mobility.[96] For the first time, Oh et al. reported the fabrication of Zn_2SnO_4 (ZSO) nanoparticle-based PSCs with a PCE of 7%.[63] Zhu et al. applied $BaSnO_3$ (BSO) nanoparticles to PSCs, achieving a PCE of 12.3%.[97] To improve the electron mobility of BSO, they incorporated La as a dopant in BSO, thereby increasing the device performance up to 15.1%.[98] However, the synthesis of ZSO and La-doped BSO (LBSO) require high temperatures above 700 °C, which is not competitive compared to binary oxides. In 2016, we designed a highly reactive precursor and successfully lowered the processing temperature of ZSO to 90 °C, developing ZSO-based flexible PSCs with a PCE of 15.3%.[99] More recently, using LBSO prepared below

300 °C, we fabricated PSCs with a PCE of 21.2% and superior long-term photostability.[100]

Although various binary and ternary metal oxides are being studied as an alternative to TiO_2, their device performance is still lower than TiO_2-based PSCs. To improve the properties of existing metal oxides, further study regarding surface modification and doping is necessary. Especially, in the case of ternary metal oxides, there are many possibilities for transforming their electrical and optical properties by partial cation substitution because they contain two cation sites. Nonetheless, their high processing temperature makes it hard to obtain a single phase of a ternary oxide with the desired composition. The development of a low-temperature synthetic method is indispensable for ternary metal oxides. Furthermore, to achieve both high efficiency and stability, much effort must be made to find promising metal oxides with superior electrical and optical properties to TiO_2, in addition to reforming the existing metal oxides.

The development of new metal oxides can be largely divided into two steps. The first step is to discover a new composition for a metal oxide with suitable properties, and the second is to adopt the proper synthetic method for the new metal oxide to exhibit high device performance.

Figure 3 shows a strategy for efficiently finding new metal oxides to be used as ETMs in PSCs. First of all, metal-oxide candidates having appropriate electronic properties are searched via a computational method based on density functional theory (DFT). As mentioned above, metal-oxide candidates for ETMs should possess favorable conduction band and valence band positions, superior electron mobility, and conductivity. From the DFT calculations, we can obtain information about the electronic structure as well as the intrinsic properties of various metal oxides such as bandgap, band structure, Fermi energy, density of states, effective mass of electron and hole, and carrier density.[101] Because DFT is based on the chemical compositions and structures of materials without the use of intervening models, it is possible to predict the electronic properties of possible combinations of binary and ternary metal oxides from the periodic table using DFT.[102] For example, Myung et al. predicted that by means of the DFT calculation, La-doping onto $BaSnO_3$ lowers the conduction band edge, leaving the valence band edge intact, which leads to favorable electron transfer from $CH_3NH_3PbI_3$ perovskite to La-doped $BaSnO_3$.[103]

Also, thin films of wide bandgap metal-oxide candidates derived from DFT computations are fabricated through vacuum-based deposition techniques such as sputtering and chemical vapor deposition (CVD). In the case of ternary metal oxides, whose exact stoichiometry is difficult to control, the pulsed laser deposition (PLD) method is advantageous to obtain the pure phase of the desired composition.[104]

The next step is to evaluate whether the properties of the deposited thin film of metal-oxide candidates are suitable or not for use as ETMs. The purpose of this step is to identify if the actual properties of the metal-oxide candidates
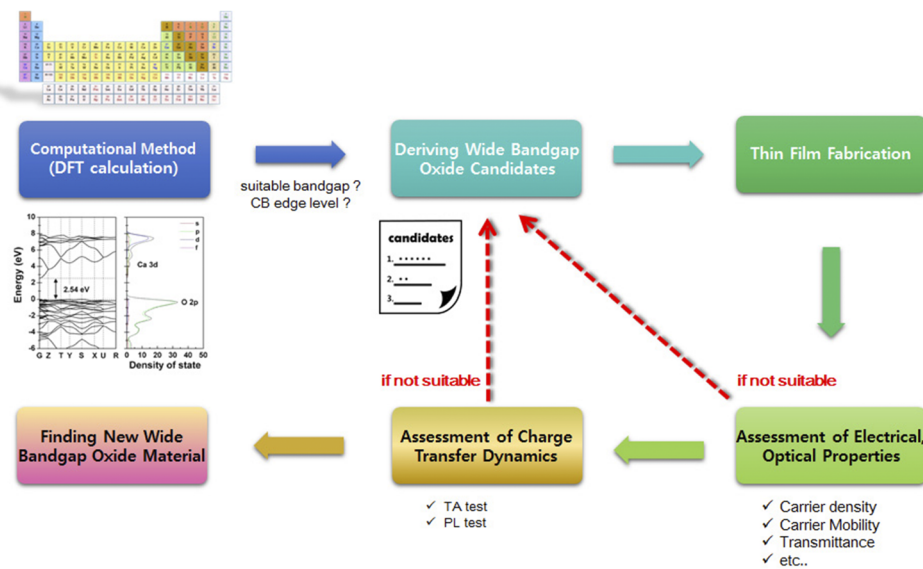
FIG. 3. Flowchart for finding a new wide bandgap metal oxide for using ETM of PSCs. (i). Computational method for searching metal oxides which have suitable electronic properties (ii). Thin film fabrication of candidates derived from theoretical calculation via sputtering, chemical vapor deposition (CVD), or pulse-laser deposition (PLD) (iii). Assessment of electrical, optical, and photophysical properties of the thin films of metal-oxide candidates.

are similar to those predicted by calculations and to pick out the final candidates with excellent characteristics among the various metal-oxide candidates. Electrical and optical properties such as bandgap, band structure, transmittance, carrier density, and carrier mobility of metal-oxide candidates can be measured through ultraviolet photoelectron spectroscopy (UPS), UV-Vis spectroscopy, and the Hall effect measurement system. Metal-oxide candidates for ETMs should have n-type characteristics, and the CBM should be lower than that of the perovskite absorber. It is desirable that the transmittance and carrier mobility of the candidates are equal to or better than those of TiO_2. After the electrical and optical properties of the metal oxide are verified, it is imperative to monitor the charge transfer dynamics at the perovskite/metal oxide interface by using transient absorption (TA) spectroscopy, time-resolved photoluminescence (TRPL), or steady-state photoluminescence (PL).[24,105] Once the charge transfer from the perovskite absorber to the metal-oxide candidate is revealed to be favorable, the basic assessment about the candidate is over. If a candidate does not satisfy a certain criterion, the candidate is excluded, and the thin film of another candidate is made and evaluated.

In developing new wide bandgap metal oxides, the selection of a synthetic process is an important factor because it can largely affect the quality of wide bandgap metal oxides, processing time, and cost. Figure 4 shows general synthetic methods of metal oxides to apply to PSCs. The wet chemical synthetic process is a very promising method for synthesis of metal oxides because of its low cost, mass production, and high yield. Sol-gel and solvothermal processes are the most widely used wet chemical techniques. The sol-gel process and solvothermal process synthesize solid crystalline oxides from small molecules, i.e., precursor solution.[106,107] To synthesize colloidal nanoparticles through the sol-gel

process, precursors including metal alkoxides and metal chlorides undergo hydrolysis and polycondensation reactions to form amorphous nanoparticles. The solvothermal process enables the preparation of crystalline nanoparticles by secondary treatment under hydrothermal conditions.[107] To apply to PSCs, the colloids can be spin-coated onto a substrate to form a dense thin film. In this case, the size, morphology, crystallinity, and dispersion of the synthesized nanoparticles greatly affect the film properties and, thus, device performance. Therefore, a strategic approach of controlling the synthesis temperature, time, and surfactant is necessary to fabricate high-performance devicesIn particular, TiO_2 and SnO_2 nanoparticulate films are widely used in PSCs, and PSCs that use them show superior device performance greater than 21%.[67,83] However, this process includes a somewhat complicated process that includes (1) a process of synthesizing high-quality colloidal nanoparticles, (2) a washing process, and (3) a process of coating the synthesized colloidal nanoparticles onto the substrate. A simpler method is to inhibit the hydrolysis and polycondensation of the precursor solution and
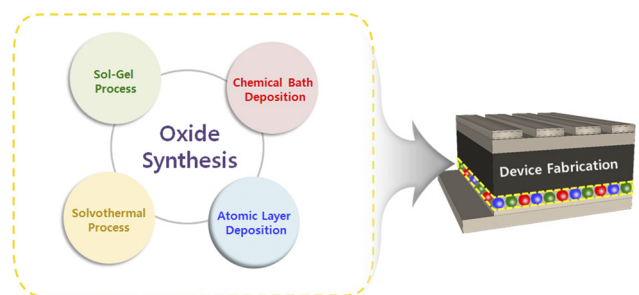
FIG. 4. General synthetic methods for wide bandgap metal oxides in PSCs.

directly coat it onto the substrate to deposit a dense thin film by thermal decomposition.[108] This method is simpler than the process using nanoparticles but has a problem in that the efficiency is lower than that of the device based on nanoparticulate films, requiring a higher processing temperature, which limits the application of flexible substrate.[108]

CBD is another good wet chemical method to deposit thin films and nanomaterials under 100 °C.[82,109] This technique directly deposits the nanoparticulate film onto a substrate by nucleation and growth mechanism. Moreover, the tuning of a reaction parameter such as duration of deposition, temperature, and pH of the solution can obtain the metal oxide film with good morphology and crystallinity for application to PSCs. Recently, some groups successfully synthesized the SnO_2 thin film through the CBD method and applied it to planar PSCs. The fabricated planar PSCs showed superior device performance greater than 21% with excellent device stability, demonstrating the potential of the CBD method.[82] However, the acidic solution for CBD chemically damages the indium-doped tin oxide (ITO) substrate, suppressing the application to flexible PSCs.

ALD, a vapor-phase technique, is another attractive method for deposition of the metal oxide thin film onto a substrate. ALD has various advantages such as precise control of the film thickness and composition and conformal coating onto a large-area substrate. In particular, the accurate control of metal oxide composition enables the deposition of various metal oxides, which have various band structures. Additionally, its low temperature process is beneficial when working with fragile or flexible polymer substrates. Recently, some researchers reported flexible PSCs fabricated by ALD with superior device performance, revealing that the ALD technique is promising in the field of PSCs.[81] However, high processing cost and long processing time remain a challenge for the ALD technique.

The optimal synthetic method can vary depending on the type of metal oxide and the intended use of the device. Therefore, a synthetic process should be carefully adopted in the process of developing wide bandgap metal oxides, considering the device efficiency, processing time, and cost.

In perspective, we reviewed the development of wide bandgap metal oxides for use in PSCs and their limitations. Wide bandgap metal oxides are a critical component affecting device performance and stability. Since 2013, various metal oxides, such as TiO_2, SnO_2, ZnO, Zn_2SnO_4, and $BaSnO_3$, have been investigated for application to PSCs. The development of such metal oxides improved the efficiency and stability of PSCs. Nevertheless, the development of devices satisfying both stability and efficiency suitable at the commercialization level is further demanded. Perovskite materials, $MAPbI_3$ and $FAPbI_3$, have a Shockley-Queisser limit greater than 30%, which indicate that there is still room to enhance the efficiency of PSCs. The effective way to reach the theoretical limit is to search for a new ETM that can minimize the V_{OC} loss with perovskite and efficiently transport the electron.

We proposed a systematic process for exploring new ETMs. Theoretical predictions and experimental validation can accelerate the finding of suitable metal oxides with perovskite. Additionally, the synthetic method should be carefully selected because it can not only maximize the properties of the explored ETM but also affect processing cost and time. Although wet chemical synthesis is inexpensive and can synthesize oxides easily, it can cause problems when it is expanded to a large area. On the other hand, the vacuum process can deposit oxide evenly over a large area, but the processing cost is high. Additionally, development of a low-temperature process enables the fabrication of flexible PSCs. Therefore, synthetic processes must also be studied along with the exploration of new metal oxides. Additionally, an understanding of the perovskite/metal oxide interface should be accompanied. Through analysis of the carrier reaction at the perovskite/metal oxide interface, better ETMs that have chemical and energetic compatibility with perovskite can be designed.

REFERENCES

[1] J. Lee, M. C. Orilall, S. C. Warren, M. Kamperman, F. J. DiSalvo, and U. Wiesner, Nat. Mater. **7**, 222 (2008).
[2] H. J. Bolink, E. Coronado, J. Orozco, and M. Sessolo, Adv. Mater. **21**, 79–82 (2009).
[3] G. Mavrou, S. Galata, P. Tsipas, A. Sotiropoulos, Y. Panayiotatos, A. Dimoulas, E. Evangelou, J. W. Seo, and C. Dieker, J. Appl. Phys. **103**, 014506 (2008).
[4] M. Gutowski, J. E. Jaffe, C.-L. Liu, M. Stoker, R. I. Hegde, R. S. Rai, and P. J. Tobin, Appl. Phys. Lett. **80**, 1897–1899 (2002).
[5] K. Takada, H. Sakurai, E. Takayama-Muromachi, F. Izumi, R. A. Dilanian, and T. Sasaki, Nature **422**, 53 (2003).
[6] V. V. Sysoev, B. K. Button, K. Wepsiec, S. Dmitriev, and A. Kolmakov, Nano Lett. **6**, 1584–1588 (2006).
[7] X. Su, Z. Zhang, and M. Zhu, Appl. Phys. Lett. **88**, 061913 (2006).
[8] D. R. Rosseinsky and R. J. Mortimer, Adv. Mater. **13**, 783–793 (2001).
[9] C.-G. Granqvist, Sol. Energy Mater. Sol. Cells **92**, 203–208 (2008).
[10] X. Yu, T. J. Marks, and A. Facchetti, Nat. Mater. **15**, 383 (2016).
[11] C. Wang, L. Yin, L. Zhang, D. Xiang, and R. Gao, Sensors **10**, 2088–2106 (2010).
[12] Z. L. Wang and J. Song, Science **312**, 242–246 (2006).
[13] A. B. Stambouli and E. Traversa, Renewable Sustainable Energy Rev. **6**, 433–455 (2002).
[14] S. Royer and D. Duprez, ChemCatChem **3**, 24–65 (2011).
[15] R. Jose, V. Thavasi, and S. Ramakrishna, J. Am. Ceram. Soc. **92**, 289–301 (2009).
[16] X. Liang, S. Bai, X. Wang, X. Dai, F. Gao, B. Sun, Z. Ning, Z. Ye, and Y. Jin, Chem. Soc. Rev. **46**, 1730–1759 (2017).

[17] M. A. Haque, A. D. Sheikh, X. Guan, and T. Wu, Adv. Energy Mater. **7**, 1602803 (2017).

[18] M. F. M. Noh, C. H. Teh, R. Daik, E. L. Lim, C. C. Yap, M. A. Ibrahim, N. A. Ludin, A. R. bin Mohd Yusoff, J. Jang, and M. A. M. Teridi, J. Mater. Chem. C **6**, 682–712 (2018).

[19] K. Mahmood, S. Sarwar, and M. T. Mehran, RSC Adv. **7**, 17044–17062 (2017).

[20] G. Yang, H. Tao, P. Qin, W. Ke, and G. Fang, J. Mater. Chem. A **4**, 3970–3990 (2016).

[21] Q. Jiang, X. Zhang, and J. You, Small **14**, 1801154 (2018).

[22] P. Zhang, J. Wu, T. Zhang, Y. Wang, D. Liu, H. Chen, L. Ji, C. Liu, W. Ahmad, and Z. D. Chen, Adv. Mater. **30**, 1703737 (2018).

[23] S. D. Stranks, G. E. Eperon, G. Grancini, C. Menelaou, M. J. Alcocer, T. Leijtens, L. M. Herz, A. Petrozza, and H. J. Snaith, Science **342**, 341–344 (2013).

[24] G. Xing, N. Mathews, S. Sun, S. S. Lim, Y. M. Lam, M. Grätzel, S. Mhaisalkar, and T. C. Sum, Science **342**, 344–347 (2013).

[25] H. J. Snaith, J. Phys. Chem. Lett. **4**, 3623–3630 (2013).

[26] J. H. Noh, S. H. Im, J. H. Heo, T. N. Mandal, and S. I. Seok, Nano Lett. **13**, 1764–1769 (2013).

[27] Y. Zhao and K. Zhu, Chem. Soc. Rev. **45**, 655–689 (2016).

[28] W. Zhang, M. Saliba, D. T. Moore, S. K. Pathak, M. T. Hörantner, T. Stergiopoulos, S. D. Stranks, G. E. Eperon, J. A. Alexander-Webber, and A. Abate, Nat. Commun. **6**, 6142 (2015).

[29] Q. Dong, Y. Fang, Y. Shao, P. Mulligan, J. Qiu, L. Cao, and J. Huang, Science **347**, 967–970 (2015).

[30] D. Shi, V. Adinolfi, R. Comin, M. Yuan, E. Alarousu, A. Buin, Y. Chen, S. Hoogland, A. Rothenberger, and K. Katsiev, Science **347**, 519–522 (2015).

[31] S. Bai, Z. Wu, X. Wu, Y. Jin, N. Zhao, Z. Chen, Q. Mei, X. Wang, Z. Ye, and T. Song, Nano Res. **7**, 1749–1758 (2014).

[32] N. J. Jeon, J. H. Noh, Y. C. Kim, W. S. Yang, S. Ryu, and S. I. Seok, Nat. Mater. **13**, 897 (2014).

[33] N. J. Jeon, J. H. Noh, W. S. Yang, Y. C. Kim, S. Ryu, J. Seo, and S. I. Seok, Nature **517**, 476 (2015).

[34] M. Saliba, T. Matsui, K. Domanski, J.-Y. Seo, A. Ummadisingu, S. M. Zakeeruddin, J.-P. Correa-Baena, W. R. Tress, A. Abate, and A. Hagfeldt, Science **354**, 206–209 (2016).

[35] W. S. Yang, B.-W. Park, E. H. Jung, N. J. Jeon, Y. C. Kim, D. U. Lee, S. S. Shin, J. Seo, E. K. Kim, and J. H. Noh, Science **356**, 1376–1379 (2017).

[36] N. J. Jeon, H. Na, E. H. Jung, T.-Y. Yang, Y. G. Lee, G. Kim, H.-W. Shin, S. I. Seok, J. Lee, and J. Seo, Nat. Energy **3**, 682 (2018).

[37] See https://www.nrel.gov/pv/assets/pdfs/pv-efficiencies-07-17-2018.pdf for National Renewable Energy Laboratory (NREL), Best Research-Cell Efficiencies Chart; accessed September 2018.

[38] N.-G. Park, M. Grätzel, T. Miyasaka, K. Zhu, and K. Emery, Nat. Energy **1**, 16152 (2016).

[39] P. Vivo, J. K. Salunke, and A. Priimagi, Materials **10**, 1087 (2017).

[40] G. S. Han, H. S. Chung, B. J. Kim, D. H. Kim, J. W. Lee, B. S. Swain, K. Mahmood, J. S. Yoo, N.-G. Park, and J. H. Lee, J. Mater. Chem. A **3**, 9160–9164 (2015).

[41] S. Guarnera, A. Abate, W. Zhang, J. M. Foster, G. Richardson, A. Petrozza, and H. J. Snaith, J. Phys. Chem. Lett. **6**, 432–437 (2015).

[42] M. Kaltenbrunner, G. Adam, E. D. Głowacki, M. Drack, R. Schwödiauer, L. Leonat, D. H. Apaydin, H. Groiss, M. C. Scharber, and M. S. White, Nat. Mater. **14**, 1032 (2015).

[43] X. Dong, X. Fang, M. Lv, B. Lin, S. Zhang, J. Ding, and N. Yuan, J. Mater. Chem. A **3**, 5360–5367 (2015).

[44] K. Domanski, J.-P. Correa-Baena, N. Mine, M. K. Nazeeruddin, A. Abate, M. Saliba, W. Tress, A. Hagfeldt, and M. Graätzel, ACS Nano **10**, 6306–6314 (2016).

[45] Y. Ogomi, K. Kukihara, S. Qing, T. Toyoda, K. Yoshino, S. Pandey, H. Momose, and S. Hayase, ChemPhysChem **15**, 1062–1069 (2014).

[46] M. M. Lee, J. Teuscher, T. Miyasaka, T. N. Murakami, and H. J. Snaith, Science **338**, 643–647 (2012).

[47] J. M. Ball, M. M. Lee, A. Hey, and H. J. Snaith, Energy Environ. Sci. **6**, 1739–1743 (2013).

[48] M. J. Carnie, C. Charbonneau, M. L. Davies, J. Troughton, T. M. Watson, K. Wojciechowski, H. Snaith, and D. A. Worsley, Chem. Commun. **49**, 7893–7895 (2013).

[49] E. Edri, S. Kirmayer, D. Cahen, and G. Hodes, J. Phys. Chem. Lett. **4**, 897–902 (2013).

[50] D. Bi, S.-J. Moon, L. Häggman, G. Boschloo, L. Yang, E. M. Johansson, M. K. Nazeeruddin, M. Grätzel, and A. Hagfeldt, RSC Adv. **3**, 18762–18766 (2013).

[51] H.-S. Kim, I. Mora-Sero, V. Gonzalez-Pedro, F. Fabregat-Santiago, E. J. Juarez-Perez, N.-G. Park, and J. Bisquert, Nat. Commun. **4**, 2242 (2013).

[52] X. Yu, S. Chen, K. Yan, X. Cai, H. Hu, M. Peng, B. Chen, B. Dong, X. Gao, and D. Zou, J. Power Sources **325**, 534–540 (2016).

[53] K. Lee, C.-M. Yoon, J. Noh, and J. Jang, Chem. Commun. **52**, 4231–4234 (2016).

[54] Y. Zhang, M. Liu, G. E. Eperon, T. C. Leijtens, D. McMeekin, M. Saliba, W. Zhang, M. de Bastiani, A. Petrozza, and L. M. Herz, Mater. Horiz. **2**, 315–322 (2015).

[55] X. Yin, Y. Guo, Z. Xue, P. Xu, M. He, and B. Liu, Nano Res. **8**, 1997–2003 (2015).

[56] A. Fakharuddin, F. Di Giacomo, I. Ahmed, Q. Wali, T. M. Brown, and R. Jose, J. Power Sources **283**, 61–67 (2015).

[57] N. Islam, M. Yang, K. Zhu, and Z. Fan, J. Mater. Chem. A **3**, 24315–24321 (2015).

[58] G. J. Meyer, ACS Nano **4**, 4337–4343 (2010).

[59] Y. Li, J. Zhu, Y. Huang, F. Liu, M. Lv, S. Chen, L. Hu, J. Tang, J. Yao, and S. Dai, RSC Adv. **5**, 28424–28429 (2015).

[60] A. Guerrero, E. J. Juarez-Perez, J. Bisquert, I. Mora-Sero, and G. Garcia-Belmonte, Appl. Phys. Lett. **105**, 133902 (2014).

[61] W. A. Laban and L. Etgar, Energy Environ. Sci. **6**, 3249–3253 (2013).

[62] S. S. Shin, W. S. Yang, E. J. Yeom, S. J. Lee, N. J. Jeon, Y.-C. Joo, I. J. Park, J. H. Noh, and S. I. Seok, J. Phys. Chem. Lett. **7**, 1845–1851 (2016).

[63] L. S. Oh, D. H. Kim, J. A. Lee, S. S. Shin, J.-W. Lee, I. J. Park, M. J. Ko, N.-G. Park, S. G. Pyo, and K. S. Hong, J. Phys. Chem. C **118**, 22991–22994 (2014).

[64] L. Liu, A. Mei, T. Liu, P. Jiang, Y. Sheng, L. Zhang, and H. Han, J. Am. Chem. Soc. **137**, 1790–1793 (2015).

[65] S. Lee, J. H. Noh, H. S. Han, D. K. Yim, D. H. Kim, J.-K. Lee, J. Y. Kim, H. S. Jung, and K. S. Hong, J. Phys. Chem. C **113**, 6878–6882 (2009).

[66] F. Zhang, W. Ma, H. Guo, Y. Zhao, X. Shan, K. Jin, H. Tian, Q. Zhao, D. Yu, and X. Lu, Chem. Mater. **28**, 802–812 (2016).

[67] H. Tan, A. Jain, O. Voznyy, X. Lan, F. P. G. de Arquer, J. Z. Fan, R. Quintero-Bermudez, M. Yuan, B. Zhang, and Y. Zhao, Science **355**, 722–726 (2017).

[68] X. Liu, Y. Zhang, L. Shi, Z. Liu, J. Huang, J. S. Yun, Y. Zeng, A. Pu, K. Sun, and Z. Hameiri, Adv. Energy Mater. **8**, 1800138 (2018).

[69] A. Hagfeldt, G. Boschloo, L. Sun, L. Kloo, and H. Pettersson, Chem. Rev. **110**, 6595–6663 (2010).

[70] A. Kojima, K. Teshima, Y. Shirai, and T. Miyasaka, J. Am. Chem. Soc. **131**, 6050–6051 (2009).

[71] H.-S. Kim, C.-R. Lee, J.-H. Im, K.-B. Lee, T. Moehl, A. Marchioro, S.-J. Moon, R. Humphry-Baker, J.-H. Yum, and J. E. Moser, Sci. Rep. **2**, 591 (2012).

[72] J. H. Heo, S. H. Im, J. H. Noh, T. N. Mandal, C.-S. Lim, J. A. Chang, Y. H. Lee, H.-j. Kim, A. Sarkar, and M. K. Nazeeruddin, Nat. Photonics **7**, 486 (2013).

[73] M. Saliba, T. Matsui, J.-Y. Seo, K. Domanski, J.-P. Correa-Baena, M. K. Nazeeruddin, S. M. Zakeeruddin, W. Tress, A. Abate, and A. Hagfeldt, Energy Environ. Sci. **9**, 1989–1997 (2016).

[74] M. A. Green, A. Ho-Baillie, and H. J. Snaith, Nat. Photonics **8**, 506–514 (2014).

[75] T. Leijtens, G. E. Eperon, S. Pathak, A. Abate, M. M. Lee, and H. J. Snaith, Nat. Commun. **4**, 2885 (2013).

[76] P. Tiwana, P. Docampo, M. B. Johnston, H. J. Snaith, and L. M. Herz, ACS Nano **5**, 5158–5166 (2011).

[77] D. Liu and T. L. Kelly, Nat. Photonics **8**, 133 (2014).

[78] Z.-L. Tseng, C.-H. Chiang, S.-H. Chang, and C.-G. Wu, Nano Energy **28**, 311–318 (2016).

[79] J. Yang, B. D. Siempelkamp, E. Mosconi, F. De Angelis, and T. L. Kelly, Chem. Mater. **27**, 4229–4236 (2015).

[80] J. Cao, B. Wu, R. Chen, Y. Wu, Y. Hui, B. W. Mao, and N. Zheng, Adv. Mater. **30**, 1705596 (2018).

[81] J. P. C. Baena, L. Steier, W. Tress, M. Saliba, S. Neutzner, T. Matsui, F. Giordano, T. J. Jacobsson, A. R. S. Kandada, and S. M. Zakeeruddin, Energy Environ. Sci. **8**, 2928–2934 (2015).

[82] E. H. Anaraki, A. Kermanpur, L. Steier, K. Domanski, T. Matsui, W. Tress, M. Saliba, A. Abate, M. Grätzel, and A. Hagfeldt, Energy Environ. Sci. **9**, 3128–3134 (2016).

[83] Q. Jiang, Z. Chu, P. Wang, X. Yang, H. Liu, Y. Wang, Z. Yin, J. Wu, X. Zhang, and J. You, Adv. Mater. **29**, 1703852 (2017).

[84] K. Mahmood, B. S. Swain, A. R. Kirmani, and A. Amassian, J. Mater. Chem. A **3**, 9051–9057 (2015).

[85] K. Wang, Y. Shi, Q. Dong, Y. Li, S. Wang, X. Yu, M. Wu, and T. Ma, J. Phys. Chem. Lett. **6**, 755–759 (2015).

[86] A. Kogo, Y. Numata, M. Ikegami, and T. Miyasaka, Chem. Lett. **44**, 829–830 (2015).

[87] M. Qin, J. Ma, W. Ke, P. Qin, H. Lei, H. Tao, X. Zheng, L. Xiong, Q. Liu, and Z. Chen, ACS Appl. Mater. Interfaces **8**, 8460–8466 (2016).

[88] X. Wang, L.-L. Deng, L.-Y. Wang, S.-M. Dai, Z. Xing, X.-X. Zhan, X.-Z. Lu, S.-Y. Xie, R.-B. Huang, and L.-S. Zheng, J. Mater. Chem. A **5**, 1706–1712 (2017).

[89] T. Minemoto and M. Murata, J. Appl. Phys. **116**, 054505 (2014).

[90] J. Wang, M. Qin, H. Tao, W. Ke, Z. Chen, J. Wan, P. Qin, L. Xiong, H. Lei, H. Yu, and G. Fang, Appl. Phys. Lett. **106**, 121104 (2015).

[91] K. Manseki, T. Ikeya, A. Tamura, T. Ban, T. Sugiura, and T. Yoshida, RSC Adv. **4**, 9652–9655 (2014).

[92] J. Dong, J. Shi, D. Li, Y. Luo, and Q. Meng, Appl. Phys. Lett. **107**, 073507 (2015).

[93] A. Bera, K. Wu, A. Sheikh, E. Alarousu, O. F. Mohammed, and T. Wu, J. Phys. Chem. C **118**, 28494–28501 (2014).

[94] Y. Okamoto and Y. Suzuki, J. Phys. Chem. C **120**, 13995–14000 (2016).

[95] A. Pang, D. Shen, M. Wei, and Z. N. Chen, ChemSusChem **11**, 424–431 (2018).

[96] G. W. Watson, J. Chem. Phys. **114**, 758–763 (2001).

[97] L. Zhu, Z. Shao, J. Ye, X. Zhang, X. Pan, and S. Dai, Chem. Commun. **52**, 970–973 (2016).

[98] L. Zhu, J. Ye, X. Zhang, H. Zheng, G. Liu, X. Pan, and S. Dai, J. Mater. Chem. A **5**, 3675–3682 (2017).

[99] S. S. Shin, W. S. Yang, J. H. Noh, J. H. Suk, N. J. Jeon, J. H. Park, J. S. Kim, W. M. Seong, and S. I. Seok, Nat. Commun. **6**, 7410 (2015).

[100] S. S. Shin, E. J. Yeom, W. S. Yang, S. Hur, M. G. Kim, J. Im, J. Seo, J. H. Noh, and S. I. Seok, Science **356**, 167–171 (2017).

[101] Q. Tang, Z. Zhou, and Z. Chen, Wiley Interdiscip. Rev.: Comput. Mol. Sci. **5**, 360–379 (2015).

[102] E. Pavarini, E. Koch, F. Anders, and M. Jarrell, in *Correlated Electrons: From Models to Materials* (Reihe Modeling and Simulation, Jülich, 2012), Chap. 2.

[103] C. W. Myung, G. Lee, and K. S. Kim, J. Mater. Chem. A **6**, 23071–23077 (2018).

[104] G. J. Exarhos and X.-D. Zhou, Thin Solid Films **515**, 7025–7052 (2007).

[105] J. S. Manser and P. V. Kamat, Nat. Photonics **8**, 737 (2014).

[106] C.-C. Wang and J. Y. Ying, Chem. Mater. **11**, 3113–3120 (1999).

[107] H. G. Yang, G. Liu, S. Z. Qiao, C. H. Sun, Y. G. Jin, S. C. Smith, J. Zou, H. M. Cheng, and G. Q. Lu, J. Am. Chem. Soc. **131**, 4078–4083 (2009).

[108] J. Yu, X. Zhao, and Q. Zhao, Thin Solid Films **379**, 7–14 (2000).

[109] P. Nair, M. Nair, V. García, O. Arenas, Y. Pena, A. Castillo, I. Ayala, O. Gomezdaza, A. Sanchez, and J. Campos, Sol. Energy Mater. Sol. Cells **52**, 313–344 (1998).